



Structures and reaction rates of the gaseous oxidation of SO_2 by an $\text{O}_3^- (\text{H}_2\text{O})_{0-5}$ cluster – a density functional theory investigation

N. Bork^{1,2,3}, T. Kurtén^{2,3,4}, M. B. Enghoff¹, J. O. P. Pedersen¹, K. V. Mikkelsen³, and H. Svensmark¹

¹National Space Institute, Technical University of Denmark, Juliane Maries Vej 30, 2100 Copenhagen Ø, Denmark

²Division of Atmospheric Sciences and Geophysics, Department of Physics, P.O. Box 64, 00014 University of Helsinki, Helsinki, Finland

³Department of Chemistry, H.C. Ørsted Institute, University of Copenhagen, Universitetsparken 5, 2100 Copenhagen Ø, Denmark

⁴Department of Chemistry, P.O. Box 55, 00014 University of Helsinki, Helsinki, Finland

Correspondence to: N. Bork (nicolai.bork@helsinki.fi)

Received: 4 October 2011 – Published in Atmos. Chem. Phys. Discuss.: 3 November 2011

Revised: 19 March 2012 – Accepted: 3 April 2012 – Published: 19 April 2012

Abstract. Based on density functional theory calculations we present a study of the gaseous oxidation of SO_2 to SO_3 by an anionic $\text{O}_3^- (\text{H}_2\text{O})_n$ cluster, $n = 0-5$. The configurations of the most relevant reactants, transition states, and products are discussed and compared to previous findings. Two different classes of transition states have been identified. One class is characterised by strong networks of hydrogen bonds, very similar to the reactant complexes. The other class is characterised by sparser structures of hydration water and is stabilised by high entropy. At temperatures relevant for atmospheric chemistry, the most energetically favourable class of transition states vary with the number of water molecules attached. A kinetic model is utilised, taking into account the most likely outcomes of the initial $\text{SO}_2\text{O}_3^- (\text{H}_2\text{O})_n$ collision complexes. This model shows that the reaction takes place at collision rates regardless of the number of water molecules involved. A lifetime analysis of the collision complexes supports this conclusion. Hereafter, the thermodynamics of water and O_2 condensation and evaporation from the product $\text{SO}_3\text{O}_2 (\text{H}_2\text{O})_n$ cluster is considered and the final products are predicted to be O_2SO_3^- and $\text{O}_2\text{SO}_3^- (\text{H}_2\text{O})_1$. The low degree of hydration is rationalised through a charge analysis of the relevant complexes. Finally, the thermodynamics of a few relevant reactions of the O_2SO_3^- and $\text{O}_2\text{SO}_3^- (\text{H}_2\text{O})_1$ complexes are considered.

1 Introduction

One of the most debated subjects within atmospheric chemistry is the mechanisms leading to cloud formation. This is due to the combination of lacking success in constructing predictive models and the high impact of clouds on a variety of atmospheric phenomena (Solomon et al., 2007). Most noticeable is the understanding and forecasting of weather and climate (Simpson and Wiggert, 2009; Rosenfeld, 2006; Spracklen et al., 2008; Carslaw et al., 2002; Marsh and Svensmark, 2000).

A known prerequisite for formation of a cloud droplet is a cloud condensation nucleus (CCN). The chemistry and physics behind CCN formation is, however, highly complex and may involve both solid and liquid phases (Nadykto et al., 2008; Pöschl, 2005), primary and secondary particles (Zhang et al., 2007; Pierce and Adams, 2006; Kazil and Lovejoy, 2005) and may be based on organic or inorganic species (De Gouw and Jimenez, 2009; Kanakidou et al., 2005). The relative flux and importance of these particle sources are still uncertain and are known to vary greatly depending on location, altitude, temperature and many other parameters. Hence, also the influence of secondary particles is disputed, but potentially important and subject to intense research (Kirkby et al., 2011; Merikanto et al., 2009; Spacklen et al., 2008).

One of the most important species involved in secondary particle formation is sulphuric acid, mainly due to its high

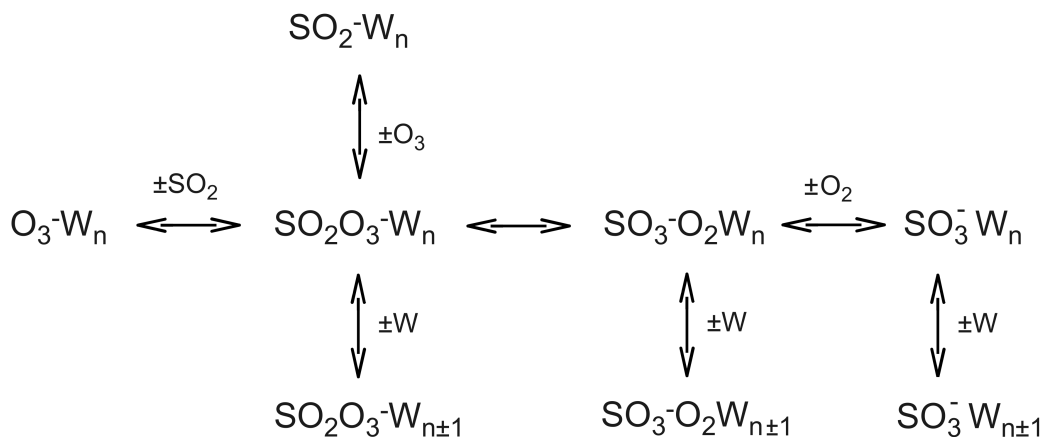


Fig. 1. Schematic overview of the investigated reactions. “W” is shorthand for water and up to 5 water molecules are here included. Under standard conditions and 50 % relative humidity, the main products are SO_3^-O_2 and $\text{SO}_3^-\text{O}_2\text{W}_1$.

water affinity (Liss and Lovelock, 2007; Charlson et al., 1987). The predominant source of atmospheric sulphuric acid is the well known UV light induced oxidation of SO_2 . Although consisting of several elementary reactions the actual sulphur oxidation step,



is believed to be rate limiting (Seinfeld and Pandis, 1998; Wine et al., 1984).

Clearly complementary to this mechanism, a number of experimental and field based studies have found correlations between cosmic rays intensities and various cloud or aerosol parameters (Kirkby et al., 2011; Svensmark et al., 2009; Enghoff and Svensmark, 2008; Harrison and Carslaw, 2003). Cosmic rays are the primary source of atmospheric ionisation and currently, ions are the most likely candidate responsible for these correlations. Although other micro- and macrophysical mechanisms may be important as well, interest have gathered around alternative mechanisms for H_2SO_4 formation involving the presence of one or more ions (Yu et al., 2008; Enghoff et al., 2012). However, the chemical and physical interactions involved in such a mechanism are still largely unresolved. The lack of knowledge of these fundamental processes is a major constraint towards the final assessment of the importance of ion induced cloud formation (Solomon et al., 2007).

Upon entrance of a cosmic ray into the atmosphere, a cascade of free electrons and various cations are produced. Although both cations and anions may be of interest for atmospheric nucleation, recently, more interest have gathered around the role of the anions and hence the fate of the electrons (Nadykto et al., 2006; Kurtén et al., 2009; Gross et al., 2008).

A free electron is thermally unstable and will most likely, rapidly attach to an O_3 molecule with a significant energy gain. The O_3^- anion has a high water affinity and will, dependent on humidity and temperature, attract a number of H_2O molecules creating a small molecular cluster. Our previous studies show that at least 5 hydration water molecules will be present at usual atmospheric conditions (Bork et al., 2011b). Any subsequent chemistry involving the $\text{O}_3^-(\text{H}_2\text{O})_n$ clusters will thus, at least initially, involve at least 5 water molecules.

The reactivity of $\text{O}_3^-(\text{H}_2\text{O})_n$ has previously been evaluated with respect to a few chemical species including CO_2 , CH_3CN , N_2O_5 , and DNO_3 (Fehsenfeld and Ferguson, 1974; Yang et al., 1991; Wincel et al., 1995, 1996). Of particular interest for sulphuric acid formation is the reaction



which has been investigated by Fehsenfeld and Ferguson (1974). The observed rate constant was determined to $1.7 \times 10^{-9} \text{ cm}^3 \text{ s}^{-1}$, close to the collision rate. However, to the best of our knowledge, no studies of Reaction (R2) has included the effect of hydration. Given our findings concerning the high water affinity of O_3^- , this should be performed for obtaining data relevant for atmospheric chemistry. Note that in both Reactions (R1) and (R2), sulfur is oxidized from S(IV) to S(V).

We have performed a density functional theory investigation of the reactivity of $\text{O}_3^-(\text{H}_2\text{O})_n$ with SO_2 , $n = 0-5$. Our main objective was to determine the reaction rate of SO_2 oxidation via this mechanism. However, a number of other possible chemical outcomes have been considered as well. These include re-evaporation of SO_2 , evaporation of O_3 and O_2 and equilibrium with water. The main reactions are illustrated in Fig. 1.

Initially, the structures of all reactants, transition states, and products are thoroughly investigated and the thermodynamics considered. Hereafter, a simple kinetic model is set up to determine the reaction rates. The distribution of the final products is evaluated and rationalised using molecular charges. Finally, a few relevant reactions of the end products are considered.

2 Computational details

Most electronic structure calculations have been performed using the Gaussian 09 package (<http://gaussian.com/>) and all relevant computational parameters are thoroughly described in a previous paper (Bork et al., 2011b). Here, a brief overview follows.

Ab initio calculations on radical systems, anionic systems, and hydrogen bonded networks require special attention with respect to several parameters in order to ensure reliable results. The extra electrons of anions are known to occupy diffuse, long ranging orbitals and hence require similar basis sets (Jensen, 2010). Also, the most common density functional theory (DFT) functionals have problems in this regard (Yanai et al., 2004). To address these issues we have utilised the CAM-B3LYP DFT functional (Yanai et al., 2004) and the aug-cc-pVDZ basis set (Dunning, 1989). The CAM-B3LYP functional is a modification to the well known B3LYP functional, including increasing Hartree-Fock exchange at increasing distances. Of further interest with respect to this study, it has been shown that CAM-B3LYP is superior to B3LYP with respect to evaluating classical activation barriers (Peach et al., 2006; Yanai et al., 2004). We have previously demonstrated excellent agreement between CAM-B3LYP/aug-cc-pVDZ and benchmark UCCSD(T)-F12/VDZ-F12 calculations (Bork et al., 2011b; Adler et al., 2007; Peterson et al., 2008). Also here, we use this method for testing the multireference character and energetics of the systems by single point calculations on CAM-B3LYP ground state structures. These calculations were performed using the MOLPRO 2010.1 package (<http://www.molpro.net/>).

The presence of multiple water molecules require a thorough sampling of configurational space. For structure optimisations we have utilised the simulated annealing technique which is able, not only to determine the nearest local minimum, but also to migrate between minima. Thereby, each calculation scans a large number of different configurations and hence, provide a much better sampling of configurational space (Corana et al., 1987).

Transition states were found using the Synchronous Transit and Quasi-Newton methods (STQN) (Peng et al., 1996) as implemented via the QST keyword. The initial guess for the transition states were obtained partly via structural analyses of the reactants and products and partly via scans of configurational space.

For analysing the charge distribution of the various clusters, we have utilised the Bader charge partitioning method (Bader, 1998, 1990). The method is based on partitioning the electronic density by zero-flux surfaces and has a much better theoretical basis than most other charge partitioning methods. Previously, this method has successfully been used to describe both charged systems (Bork et al., 2011a) and water containing systems (Henkelman et al., 2006).

3 Results and discussion

3.1 Structures and thermodynamics

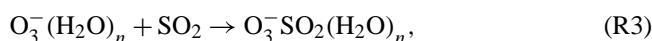
Initially, all $\text{SO}_2\text{O}_3^-(\text{H}_2\text{O})_n$, $\text{SO}_3^-\text{O}_2(\text{H}_2\text{O})_n$, and $\text{SO}_3^-(\text{H}_2\text{O})_n$ structures ($n = 0-5$) were thoroughly scanned using simulated annealing at the Hartree-Fock (HF) level. The 5–15 most stable structures were then re-optimised using DFT. In no cases were significant structural discrepancies between the most stable structures at the HF and DFT levels found.

The ground state structures of the initial collision complexes are shown in Fig. 2. In all cases, the O_3 and SO_2 molecules are found in configurations with one of the O_3 oxygen atoms clearly coordinated to the sulfur atom. The bond length is quite short, between 1.92 and 1.97 Å, indicating a relatively strong bond between the molecules. The SO_2 and O_3 molecules are thus positioned such that transferring an oxygen atom may occur without further structural rearrangement.

In the $n = 0$ and $n = 1$ cases, the remaining atoms of the O_3 molecule are turned away from the SO_2 molecule. As one more water is added, the O_3 arranges as to maximise the number of hydrogen bonds and hence, a denser configuration is obtained. Adding the 3rd, 4th and 5th water, the only noticeable difference is the coordination of the water molecules being structured in 3 and 4 membered rings.

We note that many structures are almost iso-energetic, both at 0 Kelvin and at standard conditions. Hence, we conclude that many other structures than the ones presented in Fig. 2 are found at atmospheric conditions.

Based on our previous studies, the thermodynamics of forming the collision complex, corresponding to



were hereafter readily available (Bork et al., 2011b). The Gibbs free energy potential energy surfaces are shown in Fig. 3 and tabulated in the Supplement along with enthalpy values.

All binding energies are large and positive and the $\text{SO}_2\text{O}_3^-(\text{H}_2\text{O})_n$ collision complexes are thus likely to form at atmospheric conditions. As expected, the binding energy of the SO_2 molecule is largest for small values of n . This is a consequence of the effect of the water molecules in dispersing and stabilising the charge of the O_3^- ion. This

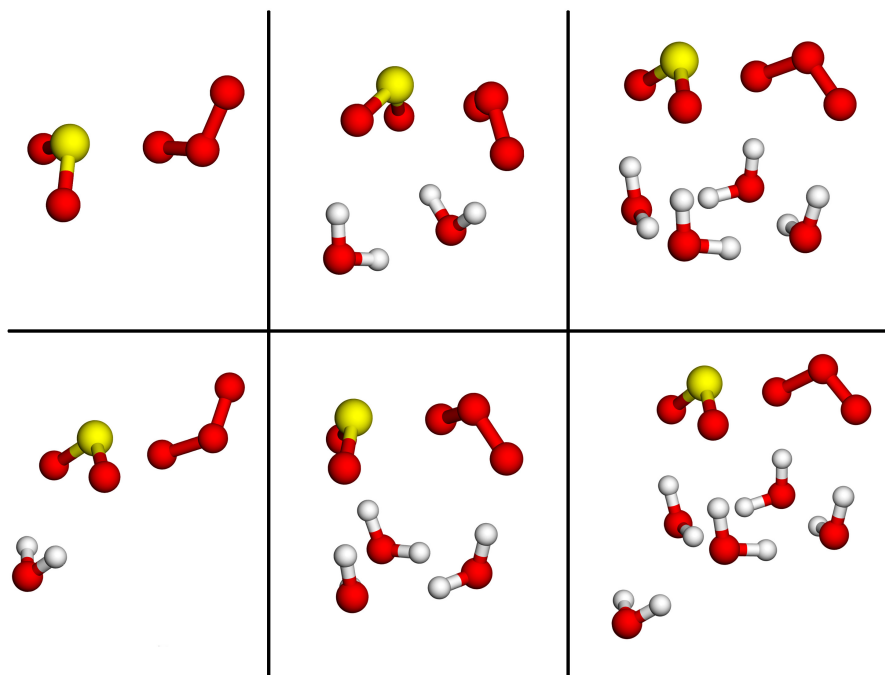


Fig. 2. Ground state structures of the initial collision complexes, $\text{SO}_2\text{O}_3^- (\text{H}_2\text{O})_n$, $n = 0-5$. For all water containing structures, a strong hydrogen bonded network is preferred. Hence, many 3 and 4 membered rings are formed. Sulfur (yellow), oxygen (red), hydrogen (white).

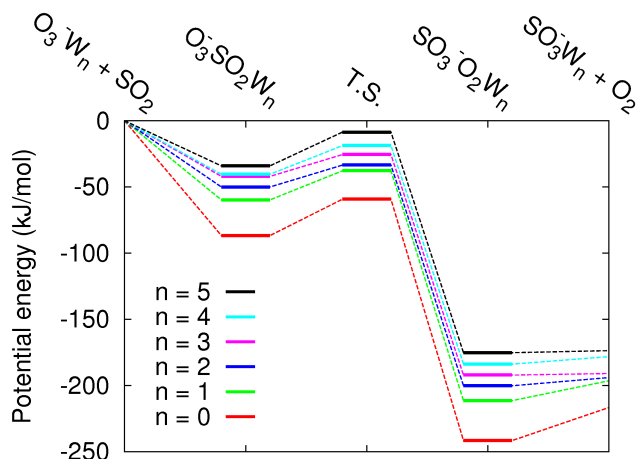
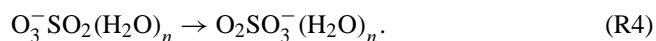


Fig. 3. Relative potential energy of the most important structures involved in the oxidation of SO_2 to SO_3 by an anionic $\text{O}_3^- (\text{H}_2\text{O})_n$ cluster, $n = 0-5$. “W” is shorthand for water. The values are tabulated in the Supplement.

stabilisation reduces the energy gain of any further clustering. Following the outline in Fig. 1, the oxygen transfer reaction was investigated,



Due to the $\text{O}_2\text{-O-SO}_2$ configuration of the reactant structures, a series of transition states were readily found and are illustrated in Fig. 4. By following the reaction coordinate in both

directions it was ensured that the transition states connected the desired reactants and products.

Minor structural differences are found, depending on the level of hydration. For $n = 0-2$, the O_3^- molecule is turned away from the SO_2 molecule, which yields a minimum S-O distance close to 1.71 Å. For $n = 3-5$, the O_3^- molecule is positioned similar to the ground state structures, inducing longer S-O distances of ca. 1.80 Å. A similar trend in the O-O bond distance is found, here referring to the bond being broken during the reaction. These are found to be around 1.69 Å and 1.75 Å for $n = 0-2$ and $n = 3-5$, respectively. In all cases, the water molecules are densely structured and this class of transition states is henceforth denoted “dense”.

Although some configurational differences are found at varying degree of hydration these are not reflected in the corresponding energy barriers, shown in Fig. 5. The free energy activation barrier for the water free system is found to 27.6 kJ mol^{-1} and is, as expected, decreased by adding the first and second water molecule. However, the addition of more water molecules tend to increase the energy barrier, i.e. stabilise the reactant complexes more than the transition states. Although ionic $\text{S}_{\text{N}}2$ reactions generally are known to proceed slower when fully solvated than in the gas phase (Olmstead and Brauman, 1977; Chabinyk et al., 1998), this is somewhat surprising since many studies have found an increasing catalytic effect of at least a few water molecules in various gas phase systems (Larson et al., 2000; Niedner-Schatteburg and Bondyby, 2000). However, in this case the

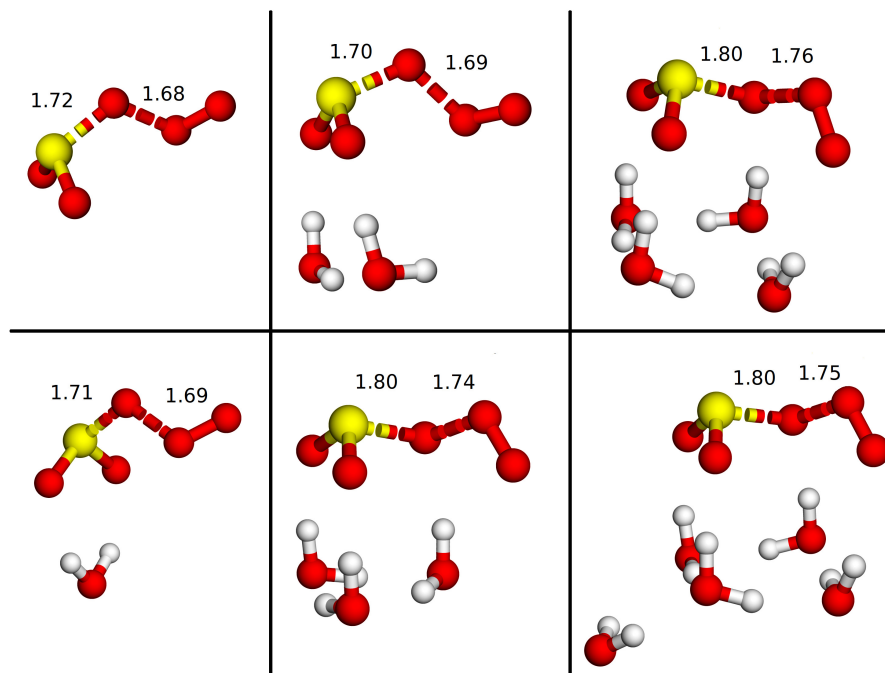


Fig. 4. Structures of the class of transition state complexes characterized by a strong network of hydrogen bonds. These are very similar to the reactant complexes, shown in Fig. 2, and are denoted “dense” due to the dense water structures. The dashed bonds indicate the bonds which are active in the reaction. Bond lengths are given in Å. Sulfur (yellow), oxygen (red), hydrogen (white).

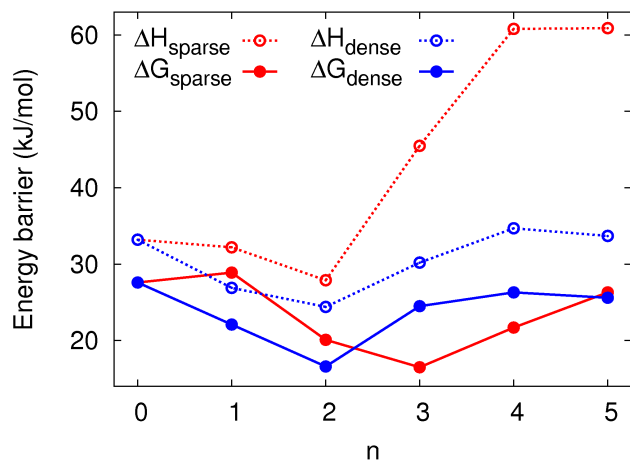


Fig. 5. ΔH and ΔG of the two classes of transition states as function of number of water molecules, n , at standard conditions. The structures of the “dense” and “sparse” transition states are shown in Figs. 4 and 6, respectively. The barrier of the charge neutral reaction is at least 58 kJ mol^{-1} for $n = 0$. The values are tabulated in the Supplement.

lowest barrier is found for the systems containing exactly 2 water molecules. We note that this is regardless of considering ΔH or ΔG within the temperature region of interest. At standard conditions, the free energy barrier is in the $n = 2$ case reduced to just 16.6 kJ mol^{-1} which is a reduction of 11 kJ mol^{-1} compared to the dehydrated structure.

While scanning configurational space, a second class of transition states was found. Within this class, the transition states are characterised by a much sparser structure of hydrogen bonds even though the configurations of the actual reactants (the $\text{O}_2\text{S-O-O}_2$ complex) are very similar. These are shown in Fig. 6 and are denoted “sparse”. Again, by following the reaction coordinate it was ensured that also these transition states connected the desired reactants and products.

Despite a much less ordered structure, the actual reactant complexes ($\text{O}_2\text{-O-SO}_2$) are more similar at varying degrees of hydration than within the “dense” class of transition states. In the “sparse” transition states, S-O distances of ca. 1.71 \AA , and O-O distances of ca. 1.69 \AA are found regardless of the number of water molecules. These distances are almost identical to the ones found in the “dense” transition states for $n = 0$ –2 and may thus be interpreted as the optimal transition state configuration at low degree of water interaction.

Examining the energy barriers of the “sparse” transition states, as expected we find the ΔH barriers significantly increased. Obviously, this occurs since the stabilisation of the hydrogen bonded network of water molecules is lost. This

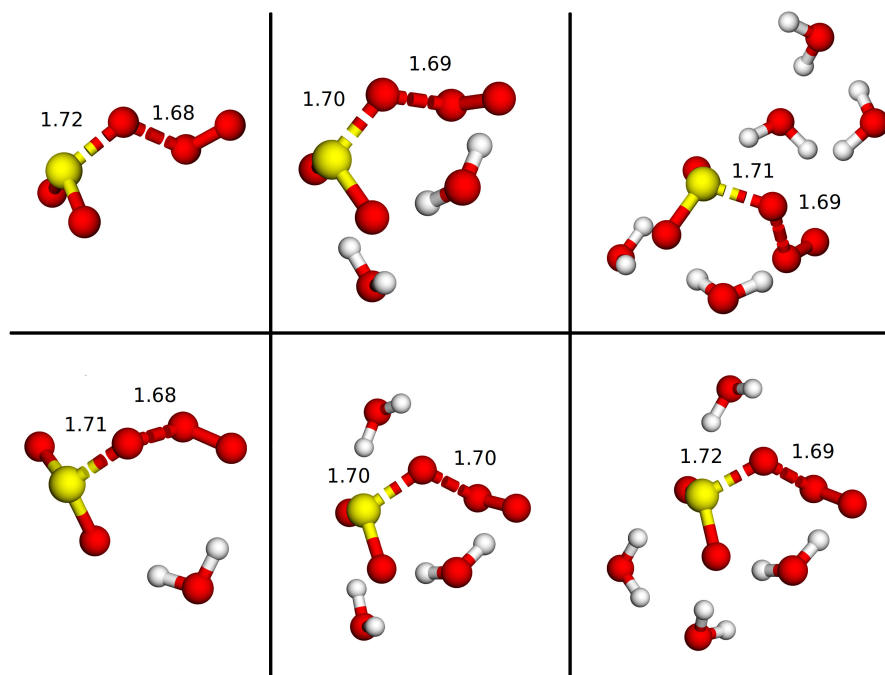


Fig. 6. Structures of the class of transition state complexes characterized by high entropy. These are denoted “sparse” due to the sparse water structures. The water free structure is again included for completeness. The dashed bonds indicate the bonds which are active in the reaction. Bond lengths are given in Å. Sulfur (yellow), oxygen (red), hydrogen (white).

is especially pronounced for $n \geq 3$, since the $n = 3$ cluster is the smallest structure capable of forming a ring of water molecules.

However, considering also entropy at standard conditions we see that the “sparse” transition states are in fact more favoured for $n = 3$ and 4. The differences are about 8 and 5 kJ mol^{-1} for $n = 3$ and 4, respectively and these “sparse” transition states are thus significantly favoured at standard conditions. Further, at $n = 5$ the values of ΔG are practically identical.

The energy barrier for the corresponding, electrically neutral reaction has been evaluated both theoretically and experimentally, albeit not including the effect of water. Using B3LYP and a triple zeta basis set, Jiang et al. (2009) determined the barrier to be around 83 kJ mol^{-1} , while Sander et al. (2006), based on time-of-flight mass spectrometry by Davis et al. (1974), suggest an activation barrier of at least 58 kJ mol^{-1} . Hence, we conclude that although the reaction may be catalysed by the presence of a few water molecules, the extra electron itself will dramatically enhance the oxidation reaction.

The structures of the product complexes were investigated as well and are shown in Fig. 7. In all cases, the same configuration of the SO_3 and O_2 molecules were found, forming an $[\text{O}_3\text{S}-\text{O}_2]^-$ complex. The S-O distances are between 1.81 and 1.85 Å and given the stability of the HSO_4^- ion, these configurations may be of relevance for the further outcome of

these complexes. At 0 Kelvin, all the most stable structures display a strong network of hydrogen bonds while other, less ordered structures become relevant at elevated temperatures. As expected, we find Reaction (R4) highly exothermic at values between 135 and 175 kJ mol^{-1} . It is thus clear that the reverse reaction will be without relevance.

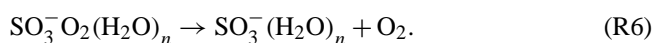
Another theoretically possible outcome of the initial collision complex is evaporation of O_3 , leaving a $\text{SO}_2^- (\text{H}_2\text{O})_n$ cluster behind. Although not performing a full simulated annealing configurational analysis of the clusters, we conclude that this reaction is at least 130 kJ mol^{-1} endothermic and hence without relevance under atmospheric conditions.

Besides discarding the relevance of O_3 evaporation from the $\text{O}_3^- \text{SO}_2 (\text{H}_2\text{O})_n$ cluster, these calculations can be used for an evaluation of the accuracy of the calculational methods. Considering the $n = 0$ systems, i.e. the reaction



we find that this is 92.1 kJ mol^{-1} endothermic. This energy equals the difference between the electron affinities of O_3 and SO_2 , given as 96 kJ mol^{-1} (Lide, 1997). This very good agreement between theoretical and experimental values is a strong argument in favour of the quality of the present results.

Finally, the structures of the $\text{SO}_3^- (\text{H}_2\text{O})_n$ clusters were examined since evaporation of O_2 is an obvious possibility,



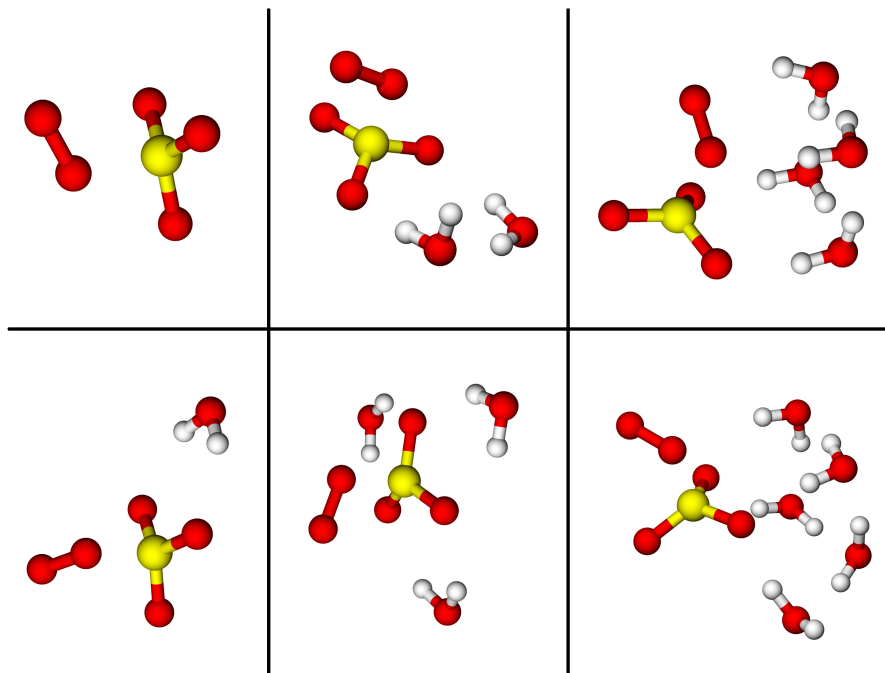
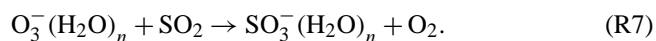


Fig. 7. Configuration of the product complexes $\text{SO}_3^-(\text{H}_2\text{O})_n$. The O_2 species is coordinated to the sulfur atom with S-O distances between 1.81 and 1.85 Å. The high concentration of atmospheric O_2 ensures a high population of these complexes. See also Sect. 3.4.

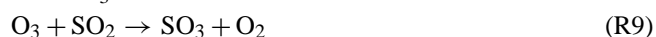
The structures were similar to the product clusters shown in Fig. 7 just without the O_2 species, and have all maintained a strong hydrogen bonded network. The structures are shown in the Supplement.

Having determined the $\text{SO}_3^-(\text{H}_2\text{O})_n$ structures and energies, the thermodynamics of O_2 evaporation was readily available. The strength of the SO_3^-O_2 bond is highly dependent of the level of hydration. The binding energy is 25 kJ mol^{-1} in the dehydrated system but only ca. 4 kJ mol^{-1} in the 5 water system. Considering the large release of internal energy due to the oxidation, the nascent O_2 molecule will have a high probability of evaporating, but given the large concentration of atmospheric O_2 , this equilibrium will quickly settle. The final product distribution is discussed in detail in Sect. 3.4.

Finally, the thermodynamics of the entire reaction chain, as illustrated in Fig. 1, are available,



Hereby, we are able to make a second assessment of the quality of the results by considering the $n = 0$ reaction as the sum of the reactions



Hereby, we can compare our value of -217 kJ mol^{-1} to the experimental ΔG° of -196 kJ mol^{-1} (Lide, 1997). Con-

sidering the inherent difficulties within DFT of describing charge transfer reactions and the potential multireference problems of O_2 and O_3 , the agreement is very satisfactory.

3.1.1 CCSD(T) calculations

Finally, CCSD(T)-F12 calculations on the isolated reactants, reactant complexes, and transition states were performed including up to two water molecules. All T1 and D1 diagnostics as well as energies are reported in the Supplement. As expected, we found rather high T1 and D1 diagnostics of ca. 0.031 and 0.16 respectively, clearly indicating partial multireference character of all reactant complexes and transition states.

Considering the energetics, distinct differences between the CAM-B3LYP and CCSD(T) energies were found. In brief, CCSD(T) predicted slightly weaker binding between the reactants in the reactant cluster, signifying a shorter lifetime towards re-evaporation of SO_2 . The differences were on the order of $5\text{--}10 \text{ kJ mol}^{-1}$ and thus within the expected range of agreement. However, the agreement concerning the height of the electronic energy barrier was significantly poorer. The CCSD(T) barriers were on the order of $4\text{--}10 \text{ kJ mol}^{-1}$ compared with the $18\text{--}24 \text{ kJ mol}^{-1}$ from CAM-B3LYP.

A better agreement between the CAM-B3LYP and CCSD(T) energies might be obtained by optimising the structures at the CCSD(T) level or increasing the basis sets for either method. However, as shall be accounted for in the following section, these seemingly significant discrepancies will not influence

the main conclusions of this study, since it will be argued that the overall reaction is diffusion limited. It should however be stressed that all of the reported energetics are to be considered qualitative rather than quantitative, both due to the mentioned discrepancies as well as the high T1 and D1 diagnostics.

3.2 Kinetics

The main objective of this study is to examine the kinetics of SO_2 oxidation to SO_3 by an $\text{O}_3^-(\text{H}_2\text{O})_n$ cluster. Having established the thermodynamic properties of the reactants, products and transition states we proceed to this point.

To determine the total rate of oxidation, steady state for the pre-reactive complex, $\text{O}_3^-\text{SO}_2(\text{H}_2\text{O})_n$, is assumed. Hereby we obtain the following set of reactions

$$\frac{d[\text{O}_3^-\text{SO}_2(\text{H}_2\text{O})_n]}{dt} = 0 \quad (1)$$

$$= Z_{\text{coll}} - r_{\text{ox}} - r_{\text{SO}_2 \text{ evap}} \quad (2)$$

where r_{ox} and $r_{\text{SO}_2 \text{ evap}}$ are the reaction rates of the oxidation and SO_2 evaporation processes, respectively. Z_{coll} is the rate of collisions leading to formation of the collision complex. Recall that evaporation of O_3 is highly endothermic and may be disregarded. At this point we consider only fixed values of n , since it later can be concluded that varying hydration will not alter the kinetics. See Sects. 3.3 and 3.4 for further analysis.

Since both r_{ox} and $r_{\text{SO}_2 \text{ evap}}$ must depend linearly on the concentration of $\text{O}_3^-\text{SO}_2(\text{H}_2\text{O})_n$ we obtain

$$Z_{\text{coll}} - [\text{O}_3^-\text{SO}_2(\text{H}_2\text{O})_n](k_{\text{ox}} + k_{\text{SO}_2 \text{ evap}}) = 0, \quad (3)$$

where “ k ” denote the corresponding rate constants.

Further, since the oxidation is highly exothermic no backwards reaction is possible and hence, the total reaction rate can be obtained as

$$r_{\text{tot}} = r_{\text{ox}} \quad (4)$$

$$= k_{\text{ox}}[\text{O}_3^-\text{SO}_2(\text{H}_2\text{O})_n] \quad (5)$$

$$= Z_{\text{coll}} \left(1 + \frac{k_{\text{SO}_2 \text{ evap}}}{k_{\text{ox}}} \right)^{-1} \quad (6)$$

where the final equation is obtained by inserting the expression for $[\text{O}_3^-\text{SO}_2(\text{H}_2\text{O})_n]$ from Eq. (3). Further assuming that both oxidation and SO_2 evaporation can be described by Arrhenius equations we obtain

$$\frac{r_{\text{tot}}}{Z_{\text{coll}}} = \left(1 + \frac{A_{\text{SO}_2 \text{ evap}}}{A_{\text{ox}}} \exp \left(- \frac{\Delta E_{\text{SO}_2 \text{ evap}} - \Delta E_{\text{ox}}}{RT} \right) \right)^{-1} \quad (7)$$

where the ratio $r_{\text{tot}}/Z_{\text{coll}}$ denote the fraction of $\text{O}_3^-\text{SO}_2(\text{H}_2\text{O})$ complexes, in which SO_2 is oxidised.

The differences in activation energies, $\Delta E_{\text{SO}_2 \text{ evap}} - \Delta E_{\text{ox}}$, are directly obtained from Fig. 3. The prefactors were obtained using transition state theory in the harmonic approximation (hTST) (Hänggi et al., 1990; Billing and Mikkelsen,

1996). The prefactor of oxidation is then given as

$$A_{\text{ox}} = \frac{\nu_{\text{react}}}{\nu_{\text{TS}}^\ddagger} \quad (8)$$

where “ ν ” denote the vibrational frequencies of the reactants and transition states. The \ddagger symbol indicate that the imaginary frequency should be omitted.

We here note that the reactant configuration, should be the first stable configuration into which the transition state falls upon relaxation and not necessarily the absolute ground state. In the class of “dense” transition states, the configuration actually relaxes into the ground state, but in the class of “sparse” transition states this is not the case. These relax into a configuration, not much different from the transition state itself.

Since evaporation of SO_2 is barrierless, there were no transition states in which to evaluate the frequencies. In stead, we loosely estimated these by gradually moving the SO_2 away from the cluster and continuously evaluating the resulting frequencies. Although this method is rough, we emphasise that the accuracy is adequate for the present purpose, namely to evaluate the fraction of reactive collisions from Eq. (7). This was ensured by a sensitivity analysis showing no major discrepancies, even considering an error of two orders of magnitude. All relevant frequencies are given in the Supplement.

Finally, we evaluate the fraction of reactive collisions at standard conditions. Regardless of the number of water molecules we find that

$$\frac{r_{\text{tot}}}{Z_{\text{coll}}} > 0.995, \quad (9)$$

i.e. practically all collisions will lead to oxidation. The main reason is not a particularly small energy barrier but rather that any other chemical fate shown in Fig. 1 requires a significantly higher activation energy.

The rate of oxidation of SO_2 by an anionic $\text{O}_3^-(\text{H}_2\text{O})_n$ cluster may thus simply be estimated using classical collision theory,

$$Z_{\text{coll}} = N_{\text{SO}_2} N_{\text{cluster}} \pi d^2 \sqrt{\frac{8k_B T}{\mu \pi}} \quad (10)$$

where N is the number of species pr. unit volume, $d = d_{\text{SO}_2} + d_{\text{cluster}}$ is the total collision cross section, k_B is Boltzmann’s constant, and μ is the reduced mass (Atkins, 2001; Billing and Mikkelsen, 1996).

Comparison with experimental data is only possible for the dehydrated system where Fehsenfeld and Ferguson (1974) measured the rate constant to $1.7 \times 10^{-9} \text{ cm}^3 \text{ s}^{-1}$ at $T = 296 \text{ K}$. In this case, considering $d = 5.5 \text{ \AA}$ obtained as a simple geometric mean of the reactants, we obtain a rate constant of $1.1 \times 10^{-10} \text{ cm}^3 \text{ s}^{-1}$. It is very plausible that the one order of magnitude difference reflects a net attractive potential between the O_3^- ion and the dipolar SO_2 increasing the collision

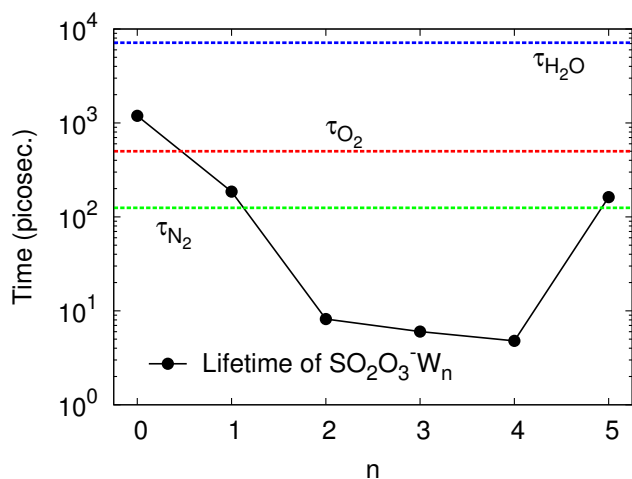


Fig. 8. Lifetime of the reactant complexes, $\text{O}_3^-\text{SO}_2(\text{H}_2\text{O})_n$ at standard conditions. For comparison, the average times between collisions, τ , with N_2 , O_2 and H_2O (50 % RH) are shown.

rates. One ion-dipole collision rate has been described by Su and Bowers (1973) and implemented by Kupiainen et al. (2011). However, these considerations are beyond the scope of this study. Alternatively, inaccuracies in the original experimental measurements may be the reason. In any case, the results are in reasonable accordance and oxidation of SO_2 by an $\text{O}_3^-(\text{H}_2\text{O})_n$ cluster is undoubtedly fast and should be considered when studying ionic atmospheric chemistry.

3.3 Lifetime of $\text{SO}_2\text{O}_3^-(\text{H}_2\text{O})_n$

Although there is no other likely fate of the isolated $\text{SO}_2\text{O}_3^-(\text{H}_2\text{O})_n$ complex other than SO_2 oxidation, collision with other atmospheric species could induce other possible end products. This is dependent of the expected lifetime of the $\text{SO}_2\text{O}_3^-(\text{H}_2\text{O})_n$ complex which was evaluated using hTST. The average lifetime, τ , is thus given as

$$\tau = \ln(2) \times k_{\text{ox}}^{-1} = \ln(2) \times A_{\text{ox}}^{-1} \times \exp\left(\frac{\Delta E_{\text{ox}}}{RT}\right) \quad (11)$$

where A_{ox} is given in Eq. (8). Hereby, the lifetimes are evaluated to be in the picosecond regime, illustrated in Fig. 8. For comparison, the average times between collisions with N_2 , O_2 and H_2O (50 % relative humidity) are illustrated as well. The values of the rate constants and lifetimes are given in the Supplement.

From this it is apparent that the most reactive complexes, i.e. the $n = 2, 3$ and 4 complexes, typically reacts before colliding with any other species. The remaining complexes will experience a few N_2 collisions and perhaps a single collision with O_2 . Collision with any other species, including H_2O is rarely experienced.

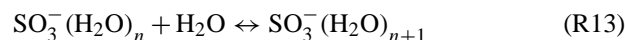
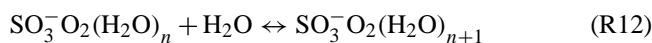
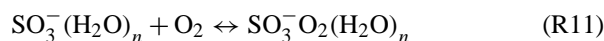
We thus conclude that the most likely fate of the $\text{SO}_2\text{O}_3^-(\text{H}_2\text{O})_n$ complex undoubtedly is SO_2 oxidation since any other outcome require a large extra activation energy and

since the complex is too short lived to experience collision with another molecule which may induce pathways not considered here.

3.4 Equilibrium with H_2O and O_2

From the previous section, the possibility of growth of $\text{SO}_2\text{O}_3^-(\text{H}_2\text{O})_n$ via stepwise water condensation has been excluded since these clusters are too short lived for the equilibrium to settle. Even though some water molecules possibly may evaporate prior to Reaction (R4), we note that this will in no way alter the overall kinetics. Regardless of the state of hydration, once the collision complex is formed no other outcome than Reaction (R4) is probable. Consequently, the degree of hydration prior to Reaction (R4) is not of primary interest.

After Reaction (R4), both the $\text{SO}_3^-\text{O}_2(\text{H}_2\text{O})_n$ and $\text{SO}_3^-(\text{H}_2\text{O})_n$ clusters will, most likely, be stable enough to reach thermal equilibrium via H_2O and O_2 evaporation and condensation. The thermodynamics of these equilibria, i.e.



are therefore considered. The energetics associated with these reactions are all available from the previous calculations and are shown in Fig. 9 along with the critical energy of cluster growth. Here exemplified for Reaction (R13), this corresponds to the value of ΔG where

$$[\text{H}_2\text{O}] \times \exp\left(-\frac{\Delta G}{RT}\right) = 1, \quad (12)$$

implying that

$$[\text{SO}_3^-(\text{H}_2\text{O})_n] = [\text{SO}_3^-(\text{H}_2\text{O})_{n+1}]. \quad (13)$$

A value of ΔG less negative than the critical clustering energy thus implies $[\text{SO}_3^-(\text{H}_2\text{O})_n] > [\text{SO}_3^-(\text{H}_2\text{O})_{n+1}]$ and vice versa. At a given set of conditions, i.e. temperature and pressure of the condensing species, the critical clustering energy thus separates the regimes of condensation and evaporation.

Considering first the equilibria with water, i.e. Reactions (R12) and (R13), we observe that the thermodynamics of water condensation is considerably weaker than expected. Although binding energies are positive for the smallest clusters, the binding energy becomes negative for condensation of the 4th and 5th water molecule. In all cases, the binding energy of H_2O to SO_3O_2^- is less negative the critical clustering energy and for the SO_3^- species, at most a few clustering water molecules will be found at atmospheric conditions.

Some experimental data are available for Reaction (R13) in the $n = 0$ and $n = 1$ case. For $n = 0$, Fehsenfeld and Ferguson (1974) and Möhler et al. (1992) determined ΔG to $-24.7 \text{ kJ mol}^{-1}$ and $-23.5 \text{ kJ mol}^{-1}$ respectively. Further,

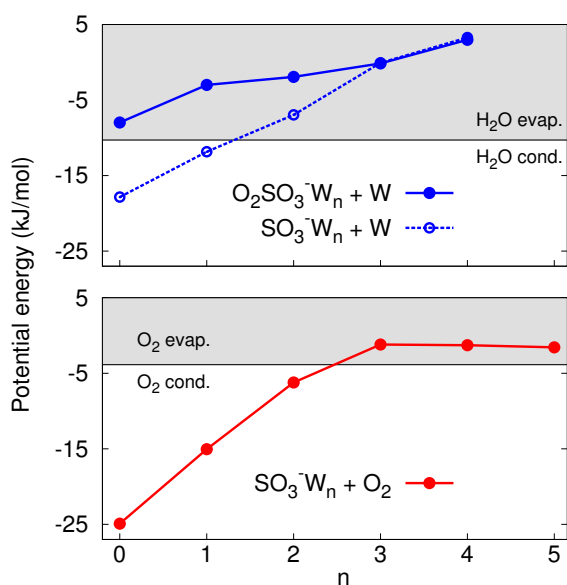


Fig. 9. Gibbs free energies of growth of the clusters via H_2O and O_2 condensation. “W” is shorthand for water. The regimes of evaporation and condensation under standard conditions and 50 % relative humidity are illustrated, determined using Eq. (13). Assuming thermal equilibrium, the final products are mainly O_2SO_3^- and $\text{O}_2\text{SO}_3^- (\text{H}_2\text{O})_1$.

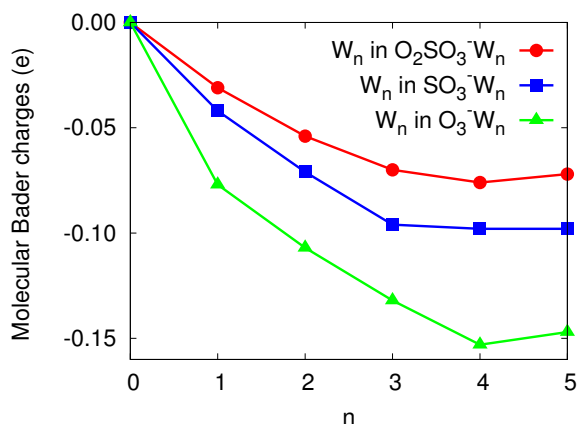


Fig. 10. Accumulated Bader charges on the water molecules (W_n) in $\text{SO}_3^- \text{O}_2$, SO_3^- and O_3^- based clusters. This charge is proportional to the binding energies and the larger the non-water part of the cluster, the less charge on the water molecules and hence, the weaker the binding.

Möhler et al. (1992) determined ΔG for the clustering of the second water molecule to $-15.5 \text{ kJ mol}^{-1}$. Finally, the first hydration energy of SO_2O_3^- was determined to $-17.2 \text{ kJ mol}^{-1}$. Considering the difficulties in describing the multireference electronic structure of the systems at hand, we conclude that the calculated energetics are in good qualitative agreement with the available experimental data although some discrepancies are found.

Considering next the equilibrium with oxygen, i.e. Reaction (R11), we see that the oxygen binding energy to the dehydrated SO_3^- anion is quite strong, but also that it quickly and smoothly converges to a value close to the critical clustering energy. To our knowledge, no direct data is available for this reaction. However, in qualitative agreement with the results presented here, both O_2SO_3^- and SO_3^- has been observed by Ehn et al. (2010) in the boreal forest at typical concentrations of up to 20 cm^{-3} and 1.5 cm^{-3} , respectively.

Assuming that the clusters reach thermal equilibrium, the final populations are readily determined using the law of mass action. Hereby, it is realised that the main product is dehydrated SO_3O_2^- . Assuming standard conditions and 50 % relative humidity, this configuration constitutes ca. 80–90 % of the resulting clusters, depending on altitude. The remaining 10–20 % of the clusters are mainly found as $\text{SO}_3^- \text{O}_2 (\text{H}_2\text{O})_1$ with any other constitution populating less than 1 %.

3.5 Charge analysis

Comparing the results of the previous section to other modelling and theoretical studies, it is surprising that the most stable configuration is without water. Most other studies on both cations and anions have found a tendency to attract at least a few water molecules at standard conditions. The best explanation is found via a molecular charge analysis of the systems, shown in Fig. 10. Included for comparison is our previous results for the O_3^- based clusters.

From this, a clear correlation between the charge and the binding energy of the water is seen. If a large amount of charge is distributed to the water molecules, proportional reductions in the electrostatic energy are obtained yielding a stronger binding energy. This is fully in line with our previous findings (Bork et al., 2011b).

It is also apparent that the size of the non-water part of the cluster is important. This is due to the extra electron being more delocalised in larger molecules, reducing the electrostatic stress on the system and hence reducing the need for further electronic delocalisation through cluster growth.

Apparently, the O_2SO_3^- cluster is almost large enough to facilitate the extra electron by itself, since only about 0.03 e is being distributed to the first water molecule. Consequently, the binding energy is just ca. 8 kJ mol^{-1} which is below the critical energy of water condensation.

3.6 Further chemistry of SO_3^-O_2

During charge neutral, photo induced, atmospheric H_2SO_4 synthesis, the rate determining step is oxidation of SO_2 to HSO_3 , shown in Reaction (R1), followed by rapid oxidation to SO_3 by O_2 (Seinfeld and Pandis, 1998; Wine et al., 1984). Once the neutral SO_3 molecule is formed, the mechanism leading to H_2SO_4 is well known and the formation is relatively fast.

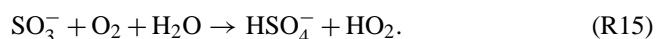
Originating from a SO_3^- based cluster, non-charged SO_3 may readily form by collision with O_3 . Considering their electron affinities, the charge transfer reaction



will be ca. 40 kJ mol^{-1} exothermic but should be studied further with respect to the effects of O_2 and H_2O (Lide, 1997). We note that formation of O_3^- may induce another SO_2 oxidation and hence, form a catalytic cycle. Exploring electronic induced catalysis in SO_3 and H_2SO_4 formation is of particular interest for explaining the observed correlations between cloud and aerosol parameters and cosmic ray influx (Kirkby et al., 2011; Svensmark et al., 2009; Enghoff and Svensmark, 2008; Harrison and Carslaw, 2003). However, the assessment of this contribution and comparing it with the dominant UV induced pathway requires that the kinetics of all reactions in the catalytic cycle are known. This work is currently ongoing.

However, the chemical fate of O_2SO_3^- may be different from neutral SO_3 and subsequently neutral H_2SO_4 . Here, we note that the species H_2SO_4^- is without atmospheric relevance since the HOMO orbital is very high in energy (NIST, 2011).

Perhaps the most obvious other outcome is synthesis of HSO_4^- via reaction with O_2 and H_2O ,



Even though this reaction is ternary and may have a significant energy barrier and complex dynamics, the necessary reactants are all abundant and therefore, this reaction is a likely candidate as well.

Naturally, HSO_4^- and H_2SO_4 are closely related and share many properties, but should Reaction (R15) occur, the catalytic effect of the electron will terminate due to the high stability of the HSO_4^- ion. The competing rates of Reactions (R14) and (R15) will thus ultimately limit how many SO_2 oxidations each free electron may induce.

4 Conclusions

The role of ion-induced H_2SO_4 formation has for a long time lacked a proper explanation of the chemical and physical mechanism. We have performed density functional theory calculations on some of the most important reactions in a proposed mechanism for ion induced SO_2 oxidation (Fig. 1).

Motivated by a previous study (Bork et al., 2011b), we find that $\text{O}_3^-(\text{H}_2\text{O})_n$ clusters are capable of further clustering with SO_2 , creating $\text{O}_3^-\text{SO}_2(\text{H}_2\text{O})_n$ clusters (Fig. 2). A variety of possible outcomes of these clusters have been examined. The most likely outcome, requiring the smallest activation energy, is oxidation of SO_2 to SO_3^- .

Two classes of transition states were identified. One characterised by a network of hydrogen bonds and one characterised by high entropy (Figs. 4 and 6). At standard conditions, both are important and will significantly contribute to the total reaction rate (Fig. 5).

Using a simple kinetic model, we determined that the reaction takes place at collision rates, in accordance with the available experimental data. Further, the lifetime of the collision complex was determined to exclude other possible outcomes, induced by collision with other reactants (Fig. 8).

Assuming thermal equilibrium, we determined the composition of the resulting products by considering their equilibrium with H_2O and O_2 (Fig. 9). Using the law of mass action, the most likely products were determined to be SO_3^-O_2 and $\text{SO}_3^-\text{O}_2(\text{H}_2\text{O})_1$ (Fig. 7) at ca. 80–90% and 10–20% population, respectively, dependent on altitude.

Finally, these results were rationalised using molecular charge analysis showing a reduced tendency of charge delocalisation for these clusters. In accordance with previous results, the degree of charge delocalisation was proportional to the binding energies and the low degree of hydration could be explained (Fig. 10).

This line of research will continue by studying the dynamics and kinetics of Reaction (R14) and thereby quantifying the atmospheric relevance of ion induced SO_2 oxidation. Also the effect of H_2O and O_2 on this reaction will be investigated. Furthermore, we wish to make future investigations concerning larger clusters and their impact on the scattering of electromagnetic radiation from the Sun and the Earth and this will be done utilizing the methods presented by Poulsen et al. (2001), Osted et al. (2004) and Jensen et al. (2000).

Supplementary material related to this article is available online at: <http://www.atmos-chem-phys.net/12/3639/2012/acp-12-3639-2012-supplement.pdf>.

Acknowledgements. The authors thank the Danish Center for Scientific Computing for access to computing facilities. Further, T. K. thanks the Academy of Finland for funding and the CSC IT Centre for Science in Espoo, Finland for computer time and M. B. E. thanks the Carlsberg Foundation for financial support. K. V. M. thanks the Danish Natural Science Research Council/The Danish Councils for Independent Research and the Villum Kann Rasmussen Foundation for financial support.

Edited by: N. M. Donahue

References

- Adler, T. B., Knizia, G., and Werner, H. J.: A simple and efficient CCSD(T)-F12 approximation, *J. Chem. Phys.*, 127, 221106, doi:10.1063/1.2817618, 2007.
- Atkins, P. and de Paula, J.: *Physical Chemistry*, 8th Edn., Oxford University Press, New York, USA, 2006.
- Bader, R. F. W.: *Atoms in molecules: a quantum theory*, Clarendon Press Oxford, Oxford University Press, Oxford, USA, 1990.
- Bader, R. F. W.: 1997 Polanyi award lecture: why are there atoms in chemistry?, *Can. J. Chemistry*, 76, 973–988, 1998.
- Billing, G. D. and Mikkelsen, K. V.: *Introduction to molecular dynamics and chemical kinetics*, Wiley, New York, USA, 1996.
- Bork, N., Bonanos, N., Rossmeisl, J., and Vegge, T.: Ab initio charge analysis of pure and hydrogenated perovskites, *J. Appl. Phys.*, 109, 033703, 2011a.
- Bork, N., Kurtén, T., Enghoff, M. B., Pedersen, J. O. P., Mikkelsen, K. V., and Svensmark, H.: Ab initio studies of $\text{O}_2^- (\text{H}_2\text{O})_n$ and $\text{O}_3^- (\text{H}_2\text{O})_n$ anionic molecular clusters, $n \geq 12$, *Atmos. Chem. Phys.*, 11, 7133–7142, doi:10.5194/acp-11-7133-2011, 2011b.
- Carlsaw, K., Harrison, R. G., and Kirkby, J.: Cosmic rays, clouds, and climate, *Science*, 298, 1732–1737, 2002.
- Chabiny, M. L., Craig, S. L., Regan, C. K., Brauman, J. I.: Gas-Phase Ionic Reactions: Dynamics and Mechanism of Nucleophilic Displacements, *Science*, 279, 1882, doi:10.1126/science.279.5358.1882, 1998.
- Charlson, R. J., Lovelock, J. E., Andreae, M. O., and Warren, S. G.: Oceanic phytoplankton, atmospheric sulphur, cloud albedo and climate, *Nature*, 326, 655–661, 1987.
- Corana, A., Marchesi, M., Martini, C., and Ridella, S.: Minimizing multimodal functions of continuous variables with the “simulated annealing” algorithm, *ACM T. Math. Software*, 13, 262–280, 1987.
- Davis, D. D., Prusaczyk, J., Dwyer, M., and Kim, P.: Stop-flow time-of-flight mass spectrometry kinetics study. Reaction of ozone with nitrogen dioxide and sulfur dioxide, *J. Phys. Chem.*, 78, 1775–1779, 1974.
- De Gouw, J. and Jimenez, J. L.: Organic aerosols in the Earth’s atmosphere, *Environ. Sci. Technol.*, 43, 7614–7618, 2009.
- Dunning, T. H. J.: Gaussian basis sets for use in correlated molecular calculations. I. The atoms boron through neon and hydrogen, *J. Chem. Phys.*, 90, 262–280, 1989.
- Enghoff, M. B. and Svensmark, H.: The role of atmospheric ions in aerosol nucleation – a review, *Atmos. Chem. Phys.*, 8, 4911–4923, doi:10.5194/acp-8-4911-2008, 2008.
- Enghoff, M. B., Bork, N., Hattori, S., Meusinger, C., Nakagawa, M., Pedersen, J. O. P., Danielache, S., Ueno, Y., Johnson, M. S., Yoshida, N., and Svensmark, H.: An isotope view on ionising radiation as a source of sulphuric acid, *Atmos. Chem. Phys. Discuss.*, 12, 5039–5064, doi:10.5194/acpd-12-5039-2012, 2012.
- Ehn, M., Junninen, H., Petäjä, T., Kurtén, T., Kerminen, V.-M., Schobesberger, S., Manninen, H. E., Ortega, I. K., Vehkamäki, H., Kulmala, M., and Worsnop, D. R.: Composition and temporal behavior of ambient ions in the boreal forest, *Atmos. Chem. Phys.*, 10, 8513–8530, 2010, <http://www.atmos-chem-phys.net/10/8513/2010/>.
- Fehsenfeld, F. C. and Ferguson, E. E.: Laboratory studies of negative ion reactions with atmospheric trace constituents, *J. Chem. Phys.*, 61, 3181–3193, 1974.
- Gross, A., Nielsen, O. J., and Mikkelsen, K. V.: From molecules to droplets, *Adv. Quantum Chem.*, 55, 355–385, 2008.
- Hänggi, P., Talkner, P., and Borkovec, M.: Reaction-rate theory: fifty years after Kramers, *Rev. Mod. Phys.*, 62, 251–341, doi:10.1103/RevModPhys.62.251, 1990.
- Harrison, R. G. and Carslaw, K. S.: Ion-aerosol-cloud processes in the lower atmosphere, *Rev. Geophys.*, 41, 1012, doi:10.1029/2002RG000114, 2003.
- Henkelman, G., Arnaldsson, A., and Jónsson, H.: A fast and robust algorithm for Bader decomposition of charge density, *Comp. Mater. Sci.*, 36, 354–360, 2006.
- Jensen, L., Astrand, P.-O., Sylvestre-Hvid, K. O., and Mikkelsen, K. V.: Frequency-dependent molecular polarizability calculated within an interaction model, *J. Phys. Chem. A*, 104, 1563–1569, 2000.
- Jensen, F.: Describing anions by density functional theory: fractional electron affinity, *J. Chem. Theory Comput.*, 6, 2726–2735, 2010.
- Jiang, S.-D., Wang, Z.-H., Zhou, J.-H., Wen, Z.-C., and Cen, K.-F.: A quantum chemistry study on reaction mechanisms of SO_2 with O_3 and H_2O_2 , *J. Zhejiang Univ.-Sc. A*, 10, 1327–1333, 2009.
- Kanakidou, M., Seinfeld, J. H., Pandis, S. N., Barnes, I., Dentener, F. J., Facchini, M. C., Van Dingenen, R., Ervens, B., Nenes, A., Nielsen, C. J., Swietlicki, E., Putaud, J. P., Balkanski, Y., Fuzzi, S., Horth, J., Moortgat, G. K., Winterhalter, R., Myhre, C. E. L., Tsigaridis, K., Vignati, E., Stephanou, E. G., and Wilson, J.: Organic aerosol and global climate modelling: a review, *Atmos. Chem. Phys.*, 5, 1053–1123, doi:10.5194/acp-5-1053-2005, 2005.
- Kazil, J. and Lovejoy, E. R.: Tropospheric ionization and aerosol production: A model study, *J. Geophys. Res.*, 109, D19206, doi:10.1029/2004JD004852, 2004.
- Kirkby, J., Curtius, J., Almeida, J., Dunne, E., Duplissy, J., Ehrhart, S., Franchin, A., Gagné, S., Ickes, L., Kürten, A., Kupc, A., Metzger, A., Riccobono, F., Rondo, L., Schobesberger, S., Tsagko-georgas, G., Wimmer, D., Amorim, A., Bianchi, F., Breitenlechner, M., David, A., Dommen, J., downward, A., Ehn, M., Flanagan, R. C., Haider, S., Hansel, A., Hauser, D., Jud, W., Junninen, H., Kreissl, F., Kvashin, A., Laaksonen, A., Lehtipalo, K., Lima, J., Lovejoy, E. R., Makhmutov, V., Mathot, S., Mikkilä, J., Minginette, P., Mogo, S., Nieminen, T., Onnela, A., Pereira, P., Petäjä, T., Schnitzhofer, R., Seinfeld, J. H., Sipilä, M., Stozhkov, Y., Stratmann, F., Tomé, A., Vanhanen, J., Viisanen, Y., Virtala, A., Wagner, P. E., Walther, H., Weingartner, E., Wex, H., Winkler, P. M., Carslaw, K. S., Worsnop, D. R., Baltensperger, U., and Kulmala, M.: Role of sulphuric acid, ammonia and galactic cosmic rays in atmospheric aerosol nucleation, *Nature*, 476, 429–435, 2011.
- Kupiainen, O., Ortega, I. K., Kurtén, T., and Vehkamäki, H.: Amine substitution into sulfuric acid – ammonia clusters, *Atmos. Chem. Phys. Discuss.*, 11, 30853–30875, doi:10.5194/acpd-11-30853-2011, 2011.
- Kurtén, T., Ortega, I. K., and Vehkamäki, H.: The sign preference in sulfuric acid nucleation, *J. Mol. Struct.-THEOCHEM*, 901, 169–173, 2009.
- Larson, L. J., Kuno, M., and Tao, F. M.: Hydrolysis of sulfur trioxide to form sulfuric acid in small water clusters, *J. Chem. Phys.*, 112, 8830–8838, 2000.

- Lide, D. R.: Handbook of Chemistry and Physics, CRC Press, Boca Raton, Florida, USA, 1997.
- Liss, P. S. and Lovelock, J. E.: Climate change: the effect of DMS emissions, *Environ. Chem.*, 4, 377–378, 2007.
- Marsh, N. D. and Svensmark, H.: Low cloud properties influenced by cosmic rays, *Phys. Rev. Lett.*, 85, 5004–5007, 2000.
- Merikanto, J., Spracklen, D. V., Mann, G. W., Pickering, S. J., and Carslaw, K. S.: Impact of nucleation on global CCN, *Atmos. Chem. Phys.*, 9, 8601–8616, 2009, <http://www.atmos-chem-phys.net/9/8601/2009/>.
- Möhler, O., Reiner, T., and Arnold, F.: The formation of SO_5^- by gas phase ion-molecule reactions, *J. Chem. Phys.*, 97, 8233–8239, 1992.
- Nadykto, A. B., Al Natsheh, A., Yu, F., Mikkelsen, K. V., and Ruuskanen, J.: Quantum nature of the sign preference in ion-induced nucleation, *Phys. Rev. Lett.*, 96, 125701, doi:10.1103/PhysRevLett.96.125701, 2006.
- Nadykto, A. B., Al Natsheh, A., Yu, F., Mikkelsen, K. V., and Herb, J.: Computational quantum chemistry: a new approach to atmospheric nucleation, *Adv. Quantum Chem.*, 55, 449–478, 2008.
- Niedner-Schatteburg, G. and Bondybey, V. E.: FT-ICR studies of solvation effects in ionic water cluster reactions, *Chem. Rev.*, 100, 4059–4086, 2000.
- NIST: Computational Chemistry Comparison and Benchmark Database, NIST Standard Reference Database Number 101, Release 15b, August 2011, edited by: Johnson III, R. D., available at: <http://cccbdb.nist.gov/>, 2011.
- Osted, A., Kongsted, J., Mikkelsen, K. V., and Christiansen, O.: Linear Response Properties of Liquid Water Calculated Using CC2 and CCSD within Different Molecular Mechanics Methods, *J. Phys. Chem. A.*, 108, 8646–8658, 2004.
- Olmstead, W. N. and Brauman, I. J.: Gas-Phase Nucleophilic Displacement Reactions, *J. Am. Chem. Soc.*, 99, 4219–4228, doi:10.1021/ja00455a002, 1977.
- Peach, M. J. G., Helgaker, T., Safek, P., Keal, T. W., Lutnæs, O. B., Tozer, D. J., and Handy, N. C.: Assessment of a Coulomb-attenuated exchange–correlation energy functional, *Phys. Chem. Chem. Phys.*, 8, 558–562, 2006.
- Peng, C., Ayala, P. Y., Schlegel, H. B., and Frisch, M. J.: Using redundant internal coordinates to optimize equilibrium geometries and transition states, *J. Comput. Chem.*, 17, 49–56, 1996.
- Peterson, K. A., Adler, T. B., and Werner, H. J.: Systematically convergent basis sets for explicitly correlated wavefunctions: The atoms H, He, B–Ne, and Al–Ar, *J. Chem. Phys.*, 128, 084102, doi:10.1063/1.2831537, 2008.
- Pierce, J. R. and Adams, P. J.: Global evaluation of CCN formation by direct emission of sea salt and growth of ultrafine sea salt, *J. Geophys. Res.*, 111, D06203, doi:10.1029/2005JD006186, 2006.
- Poulsen, T. D., Ogilby, P. R., and Mikkelsen, K. V.: Linear response properties for solvated molecules described by a combined multi-configurational self-consistent-field/molecular mechanics model, *J. Chem. Phys.* 116, 3730–3738, 2002.
- Pöschl, U.: Atmospheric Aerosols: Composition, Transformation, Climate and Health Effects, *Angew. Chem.*, 44, 7520–7540, 2005.
- Rosenfeld, D.: Aerosols, clouds, and climate, *Science*, 312, 1323–1324, 2006.
- Sander, S. P., Abbatt, J., Barker, J. R., Burkholder, J. B., Friedl, R. R., Golden, D. M., Huie, R. E., Kolb, C. E., Kurylo, M. J., Moortgat, G., Orkin, V. L., and Wine, P. H.: Chemical kinetics and photochemical data for use in atmospheric studies evaluation number 17, Pasadena, CA: Jet Propulsion Laboratory, National Aeronautics and Space Administration, available at: <http://hdl.handle.net/2014/41648>, 2006.
- Seinfeld, J. H. and Pandis, S. N.: From air pollution to climate change, *Atmospheric Chemistry and Physics*, John Wiley & Sons, New York, USA, 1326, 1998.
- Simpson, J. and Wiggert, V.: Models of precipitating cumulus towers, *Mon. Weather Rev.*, 97, 471–489, 2009.
- Solomon, S., Qin, D., Manning, M., Chen, Z., Marquis, M., Averyt, K. B., Tignor, M., and Miller, H. L.: IPCC, 2007: Climate change 2007: The physical science basis. Contribution of Working Group I to the fourth assessment report of the Intergovernmental Panel on Climate Change, Cambridge University Press, Cambridge, United Kingdom and New York, NY, USA, 2007.
- Spracklen, D. V., Bonn, B., and Carslaw, K. S.: Boreal forests, aerosols and the impacts on clouds and climate, *Philos. T. Roy. Soc. A*, 366, 4613, doi:10.1098/rsta.2008.0201, 2008.
- Su, T. and Bowers, M. T.: Theory of ion-polar molecule collisions. Comparison with experimental charge transfer reactions of rare gas ions to geometric isomers of difluorobenzene and dichloroethylene, *J. Chem. Phys.*, 58, 3027–3037, doi:10.1063/1.1679615, 1973.
- Svensmark, H., Bondo, T., and Svensmark, J.: Cosmic ray decreases affect atmospheric aerosols and clouds, *Geophys. Res. Lett.*, 36, L15101, doi:10.1029/2009GL038429, 2009.
- Spracklen, D. V., Carslaw, K. S., Kulmala, M., Kerminen, V.-M., Sihto, S.-L., Riipinen, I., Merikanto, J., Mann, G. W., Chipperfield, M. P., Wiedensohler, A., Birmili, W., and Lihavainen, H.: Contribution of particle formation to global cloud condensation nuclei concentrations, *Geophys. Res. Lett.*, 35, L06808, doi:10.1029/2007GL033038, 2008.
- Wincel, H., Mereand, E., and Castleman Jr., A. W.: Gas phase reactions of N_2O_5 with $\text{X}^-(\text{H}_2\text{O})_n$, $\text{X}=\text{O}, \text{OH}, \text{O}_2, \text{HO}_2$, and O_3 , *J. Phys. Chem.*, 99, 1792–1798, 1995.
- Wincel, H., Mereand, E., and Castleman Jr., A. W.: Gas Phase Reactions of DNO_3 with $\text{X}^-(\text{D}_2\text{O})_n$, $\text{X}=\text{O}, \text{OD}, \text{O}_2, \text{DO}_2$, and O_3 , *J. Phys. Chem.*, 100, 7488–7493, 1996.
- Wine, P. H., Thompson, R. J., Ravishankara, A. R., Semmes, D. H., Gump, C. A., Torabi, A., and Nicovich, J. M.: Kinetics of the reaction $\text{OH} + \text{SO}_2 + \text{M} \rightarrow \text{HOSO}_2 + \text{M}$. Temperature and pressure dependence in the fall-off region, *J. Phys. Chem.*, 88, 2095–2104, 1984.
- Yanai, T., Tew, D. P., and Handy, N. C.: A new hybrid exchange–correlation functional using the Coulomb-attenuating method (CAM-B3LYP), *Chem. Phys. Lett.*, 393, 51–57, 2004.
- Yang, X., Zhang, X., and Castleman Jr, A. W.: Chemistry of large hydrated anion clusters $\text{X}^-(\text{H}_2\text{O})_n$, $n = 0-59$ and $\text{X}=\text{OH}, \text{O}, \text{O}_2$, and O_3 . 2, Reaction of CH_3CN , *J. Phys. Chem.*, 95, 8520–8524, 1991.

Yu, F., Wang, Z., Luo, G., and Turco, R.: Ion-mediated nucleation as an important global source of tropospheric aerosols, *Atmos. Chem. Phys.*, 8, 2537–2554, doi:10.5194/acp-8-2537-2008, 2008.

Zhang, H., McFarquhar, G. M., Saleeby, S. M., and Cotton, W. R.: Impacts of Saharan dust as CCN on the evolution of an idealized tropical cyclone, *Geophys. Res. Lett.*, 34, L14812, doi:10.1029/2007GL029876, 2007.